

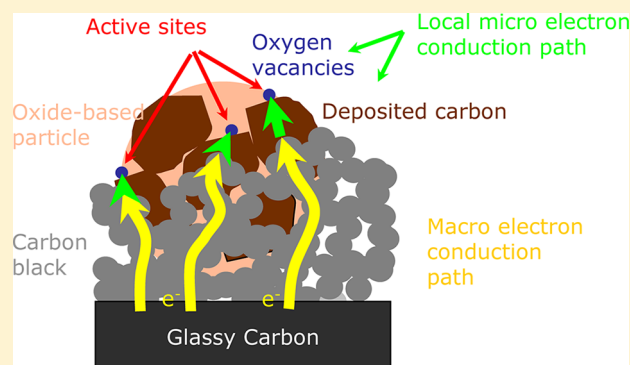
Emergence of Oxygen Reduction Activity in Partially Oxidized Tantalum Carbonitrides: Roles of Deposited Carbon for Oxygen-Reduction-Reaction-Site Creation and Surface Electron Conduction

Akimitsu Ishihara,^{*,†} Motoko Tamura,[†] Yoshiro Ohgi,^{†,§} Masashi Matsumoto,[‡] Koichi Matsuzawa,[†] Shigenori Mitsushima,[†] Hideto Imai,[‡] and Ken-ichiro Ota[†]

[†]Green Hydrogen Research Center, Yokohama National University, 79-5 Tokiwadai, Hodogaya-ku, Yokohama 240-8501, Japan

[‡]Device Functional Analysis Department, NISSAN ARC Ltd., 1 Natsushima-cho, Yokosuka 237-0061, Japan

ABSTRACT: Tantalum-oxide-based oxygen-reduction-reaction (ORR) catalysts have the ORR activity only when they are synthesized from tantalum carbonitrides. Namely pure Ta₂O₅ does not show ORR activity, and carbon or nitrogen in precursors is inevitable to form ORR active sites and to promote ORR. To clarify this reason, we investigated structural and surface electronic properties of tantalum-oxide-based catalysts, which were synthesized by gradually oxidizing tantalum carbonitride under low partial pressure of oxygen at 1000 °C, by using X-ray absorption spectroscopy, transmission electron microscopy, and Raman spectroscopy. The results indicate that oxidized tantalum carbonitrides with high ORR activity had oxygen vacancies near the surface, indicating that the vacancies could work as an active site for ORR. We also found that carbon was deposited on the oxide's surface during oxidation of tantalum carbonitrides. The deposited carbon seems to play two important roles in formation of oxygen vacancies (ORR active sites) providing reductive atmosphere, and in producing electron conduction paths on rather insulating oxides' surface.



1. INTRODUCTION

Polymer electrolyte fuel cells (PEFCs) are expected as an efficient power source used for fuel cell vehicles (FCVs) or residential cogeneration systems due to their high theoretical energy efficiency and less emission of pollutants. Because of very slow oxygen-reduction-reaction (ORR) rate, however, a large amount of platinum that promotes ORR at low temperatures must be used as a cathode catalyst in the present PEFCs. The high cost and limited recourse of platinum is a major obstacle to realize widespread commercialization of PEFCs. Although there have been many attempts to reduce the usage of Pt catalyst,¹ the drastic reduction of platinum catalysts seems to be difficult at present. Therefore, the development of new nonplatinum ORR catalysts is a central issue of this research area.

To date, many efforts have been devoted to find nonplatinum cathode catalysts, such as organometallic complexes^{2–5} and chalcogenides.^{10–12} Jasinski, first, showed that a cobalt phthalocyanine could exhibit oxygen-reduction behaviors in 35% KOH.² Jahnke and Schönborn found ORR activity of other transition metal phthalocyanines in 4.5 N H₂SO₄.³ Since then, the possibility of many other organometallic complexes has been examined.^{4,5} Alonso-Vante and Tributsch, on the other hand, found that Mo_{4.2}Ru_{1.8}Se₈ had an ORR activity in acidic media in 1986.⁶ The possibility of MM'X compounds (M

and M' = Ru, Ph, Mo, Re, Os, Fe, Cr; X = S, Se, Te) was also examined.⁷

More recently, carbon-based catalysts, such as Fe–N–C or Co–N–C, have also attracted much attention because of high ORR activity. Bashyam and Zelenay showed that the cobalt-polypyrrole composite catalyst enabled power densities of about 0.15 W cm^{–2} in H₂–O₂ fuel cells.⁸ Further, Lefevre et al. reported that iron-based catalysts exhibited similar performance of platinum supported carbon although the catalyst loading was much greater than that of Pt.⁹ Despite relatively high ORR activity of such nonplatinum electrocatalyst, the stability of these catalysts in an acid media seems to be insufficient for practical uses. Although high activity for ORR is inevitable, high stability to an acidic and oxidative atmosphere, that is, a strong corrosive environment of PEFCs' cathode, is a more important factor and an essential requirement.

Then, we have paid attention to another category of nonplatinum ORR catalysts, namely, group 4 and 5 transition-metal oxides, carbides, and oxynitrides, especially focusing on the stability of the materials in acidic electrolytes. We have reported that tungsten carbide with tantalum addition,¹⁰ tantalum oxynitride,^{11–13} zirconium oxide,^{14–16}

Received: May 28, 2013

Revised: August 13, 2013

Published: August 22, 2013

titanium oxide,¹⁷ zirconium oxynitride,^{18,19} tantalum carbonitride,²⁰ and tantalum-oxide or zirconium-oxide based catalysts,^{21–24} was stable in an acid solution and had a definite catalytic activity for the ORR.

Among them, tantalum-oxide or zirconium-oxide based catalyst exhibits extremely high activity; namely, the onset potential of ORR is more than 0.95 V vs RHE (reversible hydrogen electrode), simultaneously showing high stability in acidic conditions. These catalysts were prepared from transition metal carbonitrides, such as Ta₂CN or Zr₂CN, and partially oxidized under very low oxygen pressure.^{21–24} The ORR active sites of these catalysts are considered as oxygen-vacancy-defect sites.²⁵ Interestingly, such oxide-based catalysts show ORR activity only when they are synthesized from carbonitrides. Naturally introduced oxygen-vacancy sites or oxygen-vacancies formed via reduction atmosphere never shows ORR activity.²⁴ Carbon or nitrogen that is involved in the transition metal carbonitrides and/or slow oxidation processes using very low pressure of oxygen should be play a definitive role in emergence of ORR activity in this category of materials and elucidation of such fundamental questions should be important to design better catalysts in this category.

Then, in this paper, in order to clarify the reason why tantalum-oxide-based ORR catalysts prepared from tantalum carbonitride show the good ORR activity, we characterize Ta-CNO catalysts, which were prepared from tantalum carbonitride at 1000 °C under a low partial pressure of oxygen by X-ray absorption spectroscopy, transmission electron diffraction, Raman spectroscopy, elemental analysis, and TG-DTA measurements. The results indicate carbon is deposited on that tantalum oxide surface during the partial oxidation process of carbonitrides. Such deposited carbon plays two major roles in creation of oxygen-vacancy ORR sites and electrical conduction near the surface that promote ORR.

2. EXPERIMENTAL SECTION

2.1. Sample Preparation. The starting material, tantalum carbonitride was prepared by heating the uniform mixture of Ta₂O₅ powder and carbon black at 1600 °C under flowing N₂. A composition of the tantalum carbonitride, namely, the ratio of C and N, was controlled by a quantity of the mixed carbon black. Atomic composition of the tantalum carbonitride used as a starting material was Ta, 50.1 atom %; C, 24.7 atom %; N, 24.5 atom %; and O, 0.7 atom %. BET surface area of the Ta₂CN was 0.69 m² g^{−1}. The purity of Ta₂CN was about 99.94%.

Then, the Ta₂CN powder was heat-treated using a rotary kiln furnace at 1000 °C for several hours under a flow rate of 100 cm³ min^{−1} of the nitrogen gas containing 2% hydrogen and 0.5% oxygen to obtain catalyst powders. Because the flowing gas contained oxygen, the oxidation of carbonitride proceeded during the heat treatment. We describe the oxidized tantalum carbonitride powders as Ta-CNOs. Figure 1 shows the scheme of the synthesis of Ta₂CN and Ta-CNO.

2.2. Electrochemical Measurements. To maintain the electrical contact between the electrode and the nearly insulating Ta-CNO powders,²¹ fine Ketjenblack EC 300J powders (7 wt %) were added. The catalyst ink was made by dispersing the catalyst and Ketjenblack powder (30 mg) in 1.5 cm³ of distilled water and isopropanol (mass ratio; 1 to 1). Then, the obtained ink (ca. 2 mg) was dropped onto a glassy carbon (GC) rod (5.2 mm in diameter, Tokai Carbon Co.,

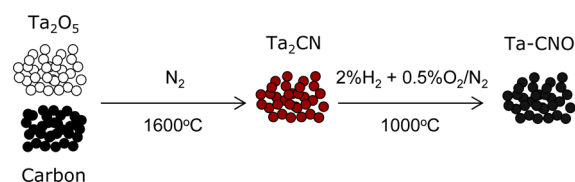


Figure 1. Scheme of synthesis of Ta₂CN and Ta-CNO.

Japan) and it was covered with 10 mm³ of 0.5 wt % recast Nafion solution.

All electrochemical experiments were performed in 0.1 mol dm^{−3} sulfuric acid at 30 °C under atmospheric pressure, using a conventional three-electrode cell that consists of a reference electrode of a reversible hydrogen electrode (RHE) and a carbon plate counter electrode. Before the evaluation of the catalytic activity, the electrode surface was cleaned by repeating cyclic voltammetry (CV) scans under oxygen at a scan rate of 1 V s^{−1} from 0.05 to 1.2 V with 100 cycles until CV reached steady state. Then, the catalytic activity for the ORR was measured by the linear scan voltammetry from 1.2 to 0.2 V at a sweep rate of 5 mV s^{−1} under oxygen or nitrogen. The ORR current (*i*_{ORR}) was determined by subtracting the current under nitrogen from that under oxygen. The onset potential for the ORR (*E*_{ORR}) was defined as the electrode potential at *i*_{ORR} = −0.2 μA cm^{−2}. A current density was based on the geometric surface area of the working electrode.

2.3. Characterization of Catalysts and Deposited Carbon. The identification of oxide-phases and crystal structure analysis of the Ta-CNO catalysts were performed by powder X-ray diffraction measurements with Cu Kα radiation.

The cross sectional images of Ta-CNO catalysts were observed using a transmission electron microscope. The specimens were prepared with focused ion beam (FIB) techniques. A high-angle annular dark-field scanning transmission electron microscopy (HAADF-STEM) observation was also performed. A transmission electron diffraction (TED) was performed to determine the crystalline structure. An electron energy-loss spectroscopy (EELS) was performed to reveal the local composition of the particle.

The local structures around Ta atoms were characterized by X-ray absorption spectroscopy (XAS) using synchrotron radiation X-rays. XAS measurements were carried out at the BL14B2 beamline at SPring-8. To obtain structural information of the near surface regions, we used conversion-electron-yield (CEY) XAS.²⁵ Since the CEY-XAS detects the flux of He⁺ ions produced by the electrons emitted from the near surface regions due to an Auger process, we can selectively analyze that local structure of near surface phases restricting the probing depth within the escape depth of the Auger electrons. The probing depth of CEY-XAS for a Ta L₃-edge was estimated to be 28.5 nm for Ta₂O₅ (density: 8.73 g cm^{−3}).²⁶

Confocal Raman spectroscopy measurements (531.95 nm laser, beam power of 0.6 mW, LabRam ARAMIS, HORIBA JOBIN YVON) was performed under ambient conditions from 100 to 2000 cm^{−1} to investigate nature of deposited carbon on the catalysts' surface.

Elemental analysis for O, N, H, and C in the catalysts was performed using an Oxygen/Nitrogen/Hydrogen Analyzer (EMGA-930, HORIBA, Japan) and a Carbon/Sulfur Analyzer (EMIA-920 V2, HORIBA, Japan).

TG-DTA measurements were carried out to monitor weight changes of the catalysts during oxidation process. Approximately 20 mg of the catalysts powder was loaded into platinum pans and heated up to 1000 °C with rate of 20 °C min⁻¹ under air.

2.4. Definition of Degree of Oxidation. We defined a parameter, DOO, as an indication of degree of oxidation by using XRD intensities for the specific reflections as previous work.²³ Typical powder X-ray diffraction patterns of Ta-CNO have both Ta₂CN and Ta₂O₅ peaks. The DOO for Ta-CNOs which contains Ta₂CN and Ta₂O₅ phases is defined as by using integrated intensity of 111 reflection of *c*-Ta₂CN and 1 11 0 reflection of *o*-Ta₂O₅.

$$\text{DOO} = \frac{I_{\text{Ta}_2\text{O}_5}}{I_{\text{Ta}_2\text{O}_5} + I_{\text{Ta}_2\text{CN}}} \quad (1)$$

A rough estimation of molar ratio of Ta₂O₅ and TaCN as a function of DOO is given in ref 25.

3. RESULTS AND DISCUSSION

3.1. Thermochemical Consideration. First, let us consider the partial oxidation process of tantalum carbonitrides from a thermochemical point of view.

Carbonitrides were heat-treated under the nitrogen gas containing 2% hydrogen and 0.5% oxygen at 1000 °C. Hydrogen reacted with oxygen to produce water, indicating that the equilibrium partial oxygen pressure of present system was very low. The equilibrium partial oxygen pressure of the present condition was calculated to be 2.77×10^{-10} Pa, namely, $\log(p_{\text{O}_2}/\text{Pa}) = -9.56$. During the oxidation of carbonitride, although the oxygen was consumed, the oxygen was continuously supplied by the dissociation of water. Therefore, the oxidation of carbonitride was continued during the heat treatment with $\log(p_{\text{O}_2}/\text{Pa})$ of -9.56 .

Figure 2 shows a phase-diagram of tantalum–carbon–nitrogen–oxygen (Ta–C–N–O) system at 1000 °C under

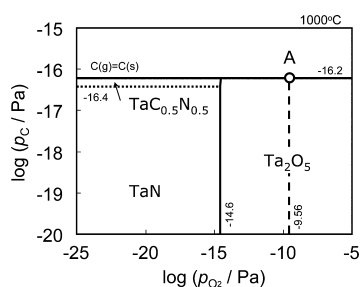


Figure 2. Phase diagram of tantalum–carbon–nitrogen–oxygen system at 1000 °C ($p_{\text{N}_2} = 101\,325$ Pa).

atmospheric pressure of nitrogen. Carbonitride was assumed to be a complete solid-solution of TaC and TaN. Nitride, carbonitride, and oxide were thermodynamically stable phases at 1000 °C. Tantalum oxide was stable above $\log(p_{\text{O}_2}/\text{Pa})$ of -14.6 .

As shown below, our Ta-CNO catalysts' surface is partially covered with carbon. It is well-known that carbon was deposited during the oxidation of carbides^{27,28} or carbonitrides as a transient reactant. Then, partial pressure of carbon should remain at $\log(p_{\text{C}}/\text{Pa}) = -16.2$ when deposited carbon existed in the system (point A in Figure 2). As oxidation time increases

such deposited carbon would be gradually oxidized and carbonitride would be completely oxidized to tantalum oxide. Such transient process, in which carbon is deposited on the partially oxidized tantalum oxides surface and such carbon is continuously oxidized, should be very important to form an ORR active "oxide" phase.

3.2. Crystal Structure Analysis of Partially Oxidized Carbonitrides. Figure 3 shows powder X-ray diffraction

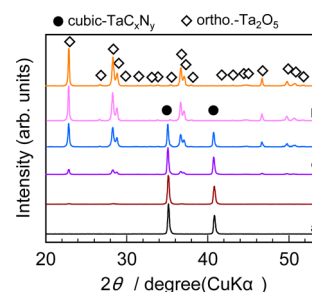


Figure 3. Powder X-ray diffraction patterns of TaC_{0.52}N_{0.48} and Ta-CNO treated at 1000 °C with DOO of 0.0 (a), 0.07 (b), 0.34 (c), 0.72 (f), 0.97 (h), and 1.0 (i) under N₂ with 2% H₂ + 0.5% O₂ gas.

patterns of Ta₂CN and Ta-CNO synthesized at 1000 °C under N₂ with 2% H₂ + 0.5% O₂ gas with DOO values of 0.0 (a), 0.07 (b), 0.34 (c), 0.72 (f), 0.97 (h), and 1.0 (i). As oxidation time increased, the DOO continuously increased. We observed only orthorhombic β -Ta₂O₅ phase as an oxide under the present condition.

3.3. ORR Activity. Figure 4 shows the potential-ORR current curves of the Ta-CNO with the DOO of 0, 0.39, and 0.96. The ORR current increased with increasing DOO.

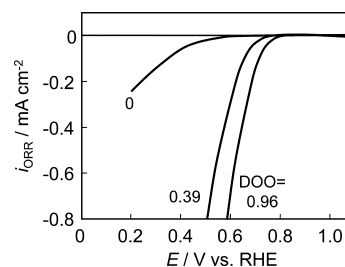


Figure 4. Potential-ORR current curves of Ta-CNO with DOO of 0, 0.39, and 0.96.

In Figure 5, we plotted the onset potential for the ORR, E_{ORR} , and the oxygen reduction reaction current, i_{ORR} at 0.6 V vs RHE, for the Ta-CNOs with respect to DOO. E_{ORR} and i_{ORR} for commercial Ta₂O₅ are also shown as reference. The starting material, Ta₂CN (DOO = 0), and commercial Ta₂O₅ (DOO = 1) showed no remarkable ORR activity: E_{ORR} of Ta₂CN and commercial Ta₂O₅ was about 0.5 V vs RHE, and i_{ORR} at 0.6 V of Ta₂CN and commercial Ta₂O₅ was not positively observed, both of which could be ascribed for the ORR from Ketjen-black that were mixed as an electrical conducting additive. The Ta-CNOs, on the other hand, exhibit clear catalytic activity for the ORR. E_{ORR} abruptly increased to 0.9 V with the increase in the DOO up to 0.2 and almost kept constant in a wide DOO range from 0.25 to 0.98. This result indicates that the active surface immediately formed by slight oxidation of Ta₂CN, and the quality of active sites did not change even if the oxidation proceeded. On the other hand, the i_{ORR} at 0.6 V gradually

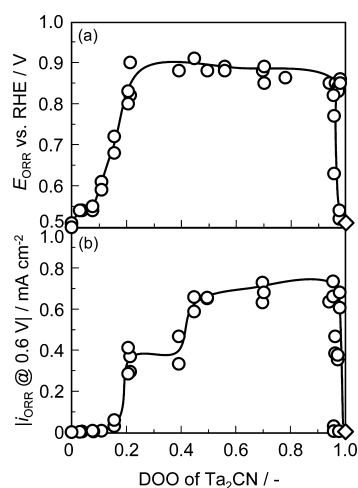


Figure 5. Onset potential toward ORR for Ta-CNO (○) and commercial Ta₂O₅ (◇) (a) and oxygen reduction current i_{ORR} at 0.6 V for Ta-CNO (○) and commercial Ta₂O₅ (◇) (b) against DOO.

increased above the DOO of 0.2. This suggests that the density of effectual active sites increased above the DOO of 0.2. In the DOO from 0.2 to 0.4, the i_{ORR} at 0.6 V was not increased. However, i_{ORR} at 0.6 V above the DOO of 0.4 increased again with the DOO.

3.4. Transmission Electron Microscopy Analyses.

Figure 6 shows TEM images and transmission electron diffraction (TED) patterns of the Ta-CNO with the DOO of 0 (a) and 0.029 (b) and electron energy-loss spectroscopy (EELS) spectra of the Ta-CNO with the DOO of 0.029. The TED spots from the inner part of the particles showed NaCl type, indicating that the inner part consists of solid solution of

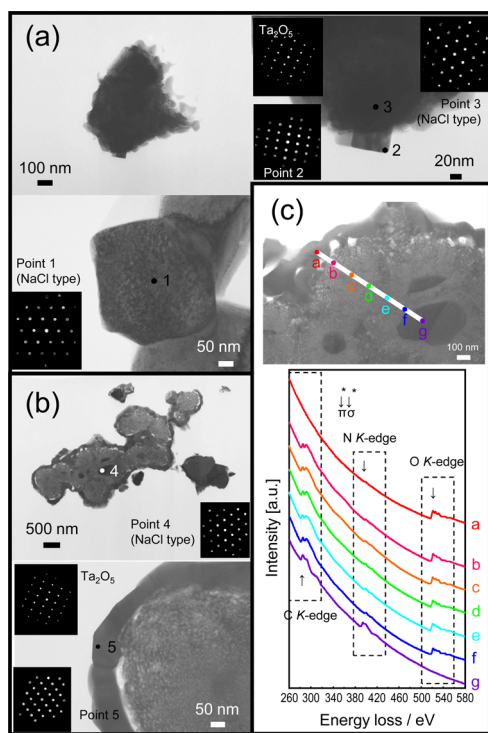


Figure 6. TEM images and Transmission Electron Diffraction (TED) patterns of Ta-CNO with DOO of 0 (a) and 0.029 (b) and EELS spectra of Ta-CNO with DOO of 0.029 (c).

TaC (JCPDS: 35-0801) and TaN (JCPDS: 49-1283). Subtle surface oxidation was observed for DOO = 0 as indicated by the TED spot that can be identified to be orthorhombic Ta₂O₅. For Ta-CNO with the DOO of 0.029, we can clearly see that the thick oxide-layer of 50–100 nm was formed near the surface region (Figure 6b).

EELS measurements were also performed to analyze the chemical compositions (C, N, and O) of the near-surface layer and inside regions. Figure 6c shows EELS spectra of the Ta-CNOs with the DOO values of 0.029. Only O was detected at point (a) on the surface layers, suggesting that surface regions consist of oxide corresponding with the TED results. Only C and O were detected in the inner regions of the surface layer at points (b) and (c), indicating that carbon is deposited on oxides in these regions. On the other hand, the phase pointed by (g) corresponded to carbonitride because both C and N were detected, and O was not detected.

3.5. Structure and Electronic Structure Analyses of Near-Surface Oxide Phase.

To analyze the local structure and electronic structure of near surface oxide-regions in the Ta-CNOs, we conducted XAS measurements in CEY mode.²⁵ Figure 7a shows the XANES spectra at Ta L_3 absorption edge

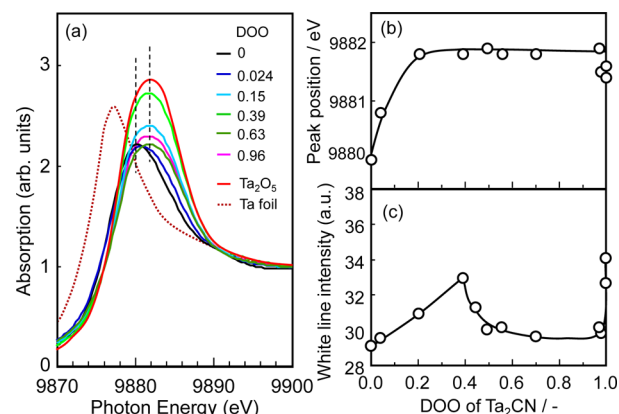


Figure 7. XANES spectra at Ta L_3 absorption edge (white line) for the Ta-CNO catalysts, taken in CEY mode (a). Dependence of peak position (b) and white line intensity (c) of XANES spectra at Ta L_3 absorption edge for Ta-CNO catalysts taken in CEY mode.

(white line) for the Ta-CNO catalysts, taken in CEY mode. Since Ta L_3 absorption arises from dipolar transition from 1s to unoccupied 5d states, the absorption (white-line intensity, peak area approximately from -5 to 10 eV from E_0 (absorption edge)) increases when the tantalum 5d band vacancy increases. We can see that the white line intensity increase as DOO increases. We note that, as DOO increase, the XANES spectra have discontinuous behavior near the DOO of 0.15.

Such behavior can be more clearly seen is the dependences of the peak position and white line intensity of the XANES spectra (Figure 7b and c). The peak position slightly increases up to DOO = 0.2, and then remains at almost the same level up to 0.98. This dependence was similar to that of the E_{ORR} on the DOO (Figure 5a). These results indicated that the surface was immediately oxidized and the surface state did not change up to DOO of 0.98.

The white line intensities, on the other hand, gradually increases up to DOO = 0.4, and then decreases from 0.4 to 0.7. Then the intensity remains at almost the same level up to 0.96 and, finally, it increases again at DOO = 1.0. This indicates that

the number of 5d band vacancies gradually decreases from 0.4 to 0.98. Comparing with DOO variations of ORR current (Figure 5b), we can conclude that density of 5d vacancies that should be related with density of oxygen-vacancy-defects correlate with ORR current.

3.6. Analysis of Deposited Carbon by Raman Spectroscopy. The formation of the oxygen vacancies seems to relate with the deposition of carbon during the oxidation of carbonitride. Figure 8 shows Raman spectra of the Ta-CNOs

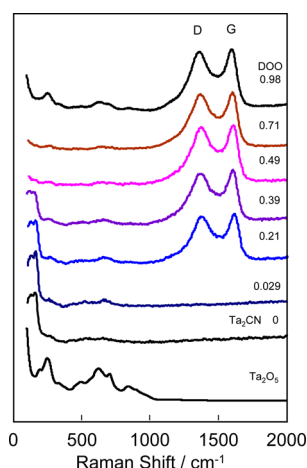


Figure 8. Raman spectra of Ta-CNOs with DOO of 0, 0.029, 0.21, 0.39, 0.49, 0.71, 0.98, and Ta₂O₅.

with the DOO of 0, 0.029, 0.21, 0.39, 0.49, 0.71, 0.98, and Ta₂O₅. Starting material with the DOO of 0, Ta₂CN, had strong peak at around 100–180 cm⁻¹. As DOO increases the broad peaks at around 500–700 cm⁻¹ that corresponds to Ta₂O₅ can be observed. And above 0.49, the Ta₂CN peaks disappear. In addition, we can see other two large peaks those are ascribed to defective graphite (G band attributed to graphitic structure at around ca. 1580 cm⁻¹ and D band attributed to defect structure at around 1330 cm⁻¹). These behaviors are a direct evidence of carbon deposition during the partial oxidation process. Since we did not observe diffraction peaks that originate in well-crystallized carbon in XRD measurements, the deposited carbon is rather amorphous. Such deposited carbon should be oxidized during partial oxidation process of carbonitrides, producing reductive atmosphere that is suitable to introduce oxygen vacancies in surface regions of tantalum oxide particles. The nature of such deposited carbon is almost independent of DOO, because the ratio of the G band to D band was unchanged from DOO = 0.21 to 0.98. Somewhat surprisingly, however, a large amount of graphitic carbon remains on the surface even DOO of 0.98, well-oxidized regions, implying an additional role of deposited carbon.

3.7. Element and Chemical Composition Analysis of Ta-CNOs during Partial Oxidation Processes. Figure 9 shows the average composition of the Ta-CNOs estimated by the results of elemental analysis for the different DOO catalysts. Because the content of hydrogen was very small (less than 0.02%), the content of H atom was omitted in Figure 9. Then, the content of tantalum was calculated by the subtracting the content of carbon, nitrogen and oxygen from the total.

Carbon or nitrogen that is contained in carbonitrides (starting materials) should play a role to create such oxygen

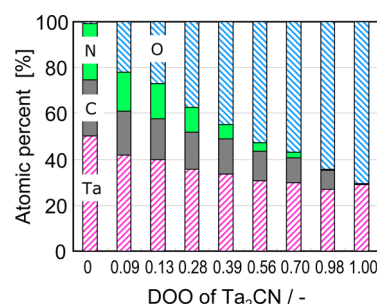
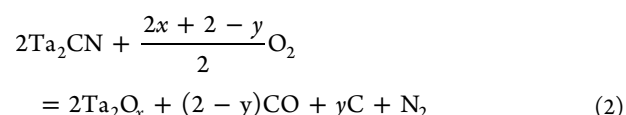


Figure 9. Average composition of Ta-CNO with different DOO (DOO = 1; commercial Ta₂O₅).

vacancies. As can be seen in Figure 9, the contents of nitrogen and carbon show different behavior to DOO. Although both the nitrogen content and carbon content decreased with the increasing DOO, the tendency of the carbon-content decrease was much smaller than that of nitrogen content. These results suggest some portion of carbon deposited on the surface.

In order to convert these relations to chemical composition (viz., ratio of Ta₂CN, Ta-oxides, deposited carbon), we first estimate O/Ta ratio in oxides. Three Ta-CNOs with the DOO of 0.98 (highly oxidized catalyst) were analyzed. The ratios of O/Ta were 2.385, 2.383, and 2.384, indicating that average composition of the bulk Ta-CNO with the DOO of 0.98 was Ta₂O_{4.77}. This result indicates that catalytically active Ta-CNO catalysts truly have oxygen vacancies.

The carbon content shown in Figure 9 contained the carbon deposited on the surface and carbon that involved in carbonitrides. Then, we tried to separate above carbon content by the following three assumptions: All remaining nitrogen exists in the form of Ta₂CN. Carbon exists as both Ta₂CN and deposited carbon. And Ta₂CN was oxidized as the following equation:



The amount of the deposited carbon was calculated by the subtracting content of the carbon that is involved in Ta₂CN from the amount of the detected carbon.

Figure 10 shows the relationship between the estimated content of compounds such as Ta₂CN, deposited C, and Ta₂O_{4.77} with respect to DOO. The amount of tantalum in Ta₂O_{4.77} was calculated by subtracting the amount of tantalum in carbonitride from the estimated amount of total tantalum.

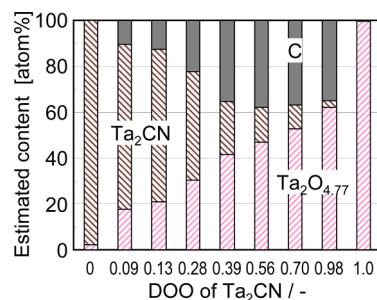


Figure 10. Relationship between estimated content of compounds such as Ta₂CN, deposited C, and Ta₂O_{4.77} and DOO.

The oxygen content calculated from $\text{Ta}_2\text{O}_{4.77}$ was well corresponded to the detected oxygen.

During partial oxidation process, in which ORR active Ta-CNOs are formed, first, the starting material Ta_2CN was oxidized to $\text{Ta}_2\text{O}_{4.77}$ as the DOO increased. Carbon was deposited above the DOO of 0.09, and the content increased as the DOO increased up to 0.56 (C: 36–37 atom %). At the DOO was 0.98, the deposited carbon remained about 35 atom %. Deposited carbon on the surface could have another role to promote ORR.

3.8. TG-DTA Analysis of Ta-CNOs. Figure 11 shows the TG and DTA curves of the Ta-CNOs with the DOO of 0, 0.04, 0.04,

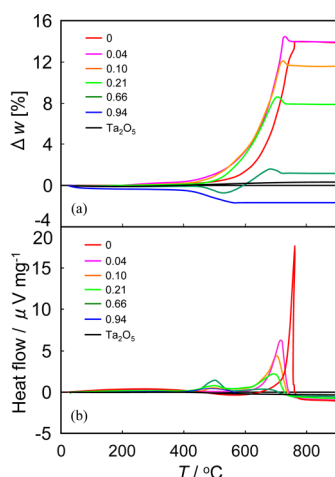
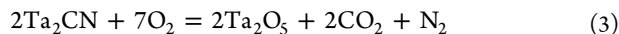


Figure 11. TG (a) and DTA (b) curves of the Ta-CNOs with DOO of 0, 0.04, 0.10, 0.21, 0.66, 0.94, and 1 under air; $10\text{ }^{\circ}\text{C min}^{-1}$.

0.10, 0.21, 0.66, 0.94, and 1 under air. Ta_2CN (DOO = 0) was oxidized to oxide above $450\text{ }^{\circ}\text{C}$ under air. The main weight increase should be related with oxidation of carbonitrides as the following equation;



As shown in both TG and DTA curves, the Ta-CNOs with small DOO values, were oxidized at lower temperatures around $400\text{ }^{\circ}\text{C}$, indicating that these were easier to oxidize than pure Ta_2CN . The additional small peaks were observed before the complete oxidation (near $700\text{ }^{\circ}\text{C}$) for the Ta-CNOs with the DOO of 0.04, 0.10, 0.21, and 0.66. The peaks could be ascribed for the carbon deposition and the oxidation of the deposited carbon. The TG curve of the Ta-CNO with the DOO of 0.66 decreased at around $420\text{ }^{\circ}\text{C}$, and then increased. The decrease was due to the oxidation of the deposited carbon, and the increase was attributed to the formation of the oxide by the oxidation of carbonitride. The oxidation behavior of deposited carbon is more clearly seen in the TG curve of the Ta-CNO with the DOO of 0.94, because it consists of tantalum oxide and deposited carbon, without carbonitride. We can see that the weight loss started at around $400\text{ }^{\circ}\text{C}$, indicating that the deposited carbon was oxidized at around $400\text{ }^{\circ}\text{C}$.

Figure 12 shows the total weight changes of the complete oxidation of the Ta-CNOs with different DOO. In Figure 12, the circle plots were obtained by TG under air. On the other hand, triangle plots were calculated from the complete oxidation of the compounds (see the following equations) whose estimated content was shown in Figure 10.

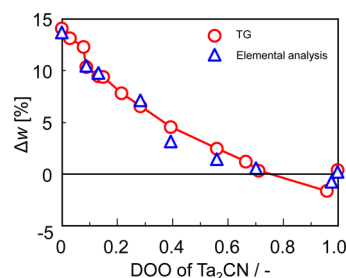
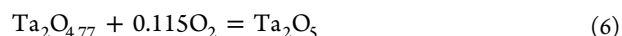
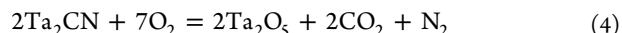


Figure 12. Total weight changes of complete oxidation of Ta-CNOs with different DOO.



Although middle values of the DOO were slightly different from the TG value, these plots corresponded well with each other. This correspondence indicated that the estimated content of compounds such as Ta_2CN , deposited C, and $\text{Ta}_2\text{O}_{4.77}$ was relatively appropriate.

3.9. Partial Oxidation Process of Ta-CNOs As Revealed TG-DTA and Chemical Analyses. Figure 13 shows the DOO dependence of the content of the related compounds and the DOO variation of C-content during oxidation, considering above experimental results.

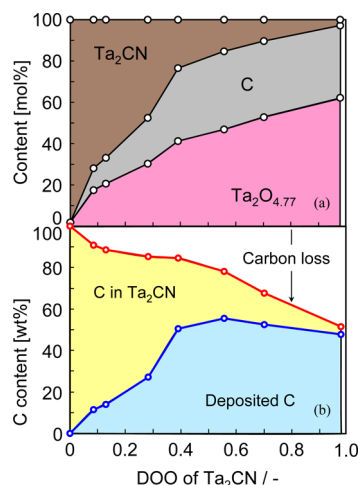


Figure 13. Dependence of estimated content of compounds such as Ta_2CN , deposited C, and $\text{Ta}_2\text{O}_{4.77}$ on DOO (a) and dependence of C content on DOO (b).

As oxidation starts, Ta_2CN gradually oxidized to tantalum oxides and solid carbon simultaneously deposits on the surface of oxides. As DOO increases, deposited carbon would be oxidized to CO and/or CO_2 . (A half of C in Ta_2CN is deposited and the rest of C oxidized at DOO = 0.2, for example.) The amount of deposited carbon increases up to DOO = 0.4. Above 0.4, deposited carbons are cautiously oxidized to CO and/or CO_2 .

The produced CO reductive atmosphere should introduce oxygen vacancies on the oxide surface. As shown in Figure 7b, white-line intensity of Ta- L_3 XANES initially increases, but above DOO = 0.4, it decreases. This behavior indicates that tantalum oxide formed at initial stage of oxidation below 0.2

have little oxygen-vacancies, while for tantalum oxide formed above DOO = 0.4, the oxide has enough vacancies to produce ORR activity. Namely, below DOO = 0.2, presumably, because the amount of deposited carbon is small thus the reductive CO density is small. Thus, the oxygen-vacancies are not introduced so much. But above 0.2, because many carbons are oxidized, the local reduction atmosphere is enough to reduce the oxides.

Another role of deposited carbon is to enhance electrical conduction on the catalyst surface. As seen in Figure 7b, since white-line intensity is almost unchanged at DOO range from 0.4 to 0.96, the number of ORR active sites (oxygen-vacancies) is almost same in this region. Indeed, E_{ORR} is almost constant in this region. On the other hand, i_{ORR} gradually increases from 0.4 to 0.98. This indicates that deposited carbon plays a role to support local electrical conduction near the ORR active sites.

5. CONCLUSIONS

In conclusion, to clarify the reason why tantalum-oxide-based ORR catalysts prepared from tantalum carbonitride show the good ORR activity, we performed various analyses such as XAS, transmission electron microscopy (TED, EELS), chemical composition, Raman spectroscopy, and TG-DTA measurements for Ta-CNOs synthesized at 1000 °C.

The results of XAS measurements indicate that in-gap states are produced by oxygen-vacancies, which can work as ORR active sites. The results of TEM, Raman, and chemical composition analysis revealed formation of deposited carbon on the oxide surface. As indicated by TG-DTA analysis, such deposited carbon produces local reductive atmosphere near the oxide surface, and plays a role to create ORR active oxygen-vacancy sites. Deposited carbon also plays a role to promote ORR by providing local nanoscale conduction paths on rather insulating oxide surfaces.

AUTHOR INFORMATION

Corresponding Author

*Phone: + 81 45 339 4021. Fax: +81 45 339 4021. E-mail: a-ishi@ynu.ac.jp.

Present Address

[§]Y.O.: Kumamoto Industrial Research Institute, Kumamoto, 862-0901, Japan.

Notes

The authors declare no competing financial interest.

ACKNOWLEDGMENTS

The authors wish to thank A.L.M.T. Corp. for supply of the Ta-CN, Dr. Yasushi Nakata (Horiba Ltd.) for Raman spectroscopy, and Dr. Satoshi Yotsuhashi and Dr. Yuka Yamada (Panasonic Corporation) for TEM and EELS measurements. The synchrotron experiments, the transmission XAS, and CEY-XAS measurements were carried out on the BL16B2 and BL14B2 beamlines at SPring-8 under approval from the Japan Synchrotron Radiation Research Institute (JASRI) (Proposal Nos. 2008B5392, 2009A5391, 2009B5390, 2008A1892, 2008B1850, 2009A1803, and 2009B1821). This work was performed under the "Non-precious metal oxide-based cathode for PEFC Project" supported by the New Energy and Industrial Technology Development Organization (NEDO).

REFERENCES

(1) Carpenter, M. K.; Moylan, T. E.; Kukreja, R. S.; Atwan, M. H.; Tessema, M. M. Solvothermal Synthesis of Platinum Alloy Nano-

particles for Oxygen Reduction Electrocatalysis. *J. Am. Chem. Soc.* **2012**, *134*, 8535–8542.

(2) Jasinski, R. A new Fuel Cell Cathode Catalyst. *Nature* **1964**, *201*, 1212–1213.

(3) Jahnke, H.; Schönborn, M. Zur Kathodischen reduktion von Sauerstoff an Phthalocyanin-Kohle-Katalysatoren. *Comptes Rendus, Troisièmes Journées Internationales d'Etude des Piles à Combustible*, 60; Presses Académiques Européennes: Bruxelles, **1969**, pp 60–65.

(4) Bezerra, C. W.B.; Zhang, L.; Lee, K.; Liu, H.; Marques, A. L.B.; Marques, E. P.; Wang, H.; Zhang, J. A Review of Fe–N/C and Co–N/C Catalysts for the Oxygen Reduction Reaction. *Electrochim. Acta* **2008**, *53*, 4937–4951.

(5) Jaouen, F.; Goellner, V.; Lefèvre, M.; Herranz, J.; Proietti, E.; Dodelet, J. P. Oxygen Reduction Activities Compared in Rotating-Disk Electrode and Proton Exchange Membrane Fuel Cells for Highly Active Fe–N–C Catalysts. *Electrochim. Acta* **2013**, *87*, 619–628.

(6) Alonso-Vante, N.; Tributsch, H. Energy Conversion Catalysis Using Semiconducting Transition Metal Cluster Compounds. *Nature* **1986**, *323*, 431–432.

(7) Feng, Y.; Gago, A.; Timperman, L.; Alonso-Vante, N. Chalcogenide Metal Centers for Oxygen Reduction Reaction: Activity and Tolerance. *Electrochim. Acta* **2011**, *56*, 1009–1022.

(8) Bashyam, R.; Zelenay, P. A Class of Non-Precious Metal Composite Catalysts for Fuel Cells. *Nature* **2006**, *443*, 63–66.

(9) Lefevre, M.; Proietti, E.; Jaouen, F.; Dodelet, J. P. Iron-Based Catalysts with Improved Oxygen Reduction Activity in Polymer Electrolyte Fuel Cells. *Science* **2009**, *324*, 71–74.

(10) Lee, K.; Ishihara, A.; Mitsushima, S.; Kamiya, N.; Ota, K. Stability and Electrocatalytic Activity for Oxygen Reduction in WC +Ta catalyst. *Electrochim. Acta* **2004**, *49*, 3479–3485.

(11) Ishihara, A.; Lee, K.; Doi, S.; Mitsushima, S.; Kamiya, N.; Hara, M.; Domen, K.; Fukuda, K.; Ota, K. Tantalum Oxynitride for a Novel Cathode of PEFC. *Electrochim. Solid-State Lett.* **2005**, *8*, A201–A203.

(12) Ishihara, A.; Doi, S.; Mitsushima, S.; Ota, K. Tantalum (Oxy)nitrides Prepared Using Reactive Sputtering for New Cathodes of Polymer Electrolyte Fuel Cell. *Electrochim. Acta* **2008**, *53*, 5442–5450.

(13) Kikuchi, K.; Ishihara, A.; Matsuzawa, K.; Mitsushima, S.; Ota, K. Tantalum-based Compounds Prepared by Reactive Sputtering as a New Non-Platinum Cathode for PEFC. *Chem. Lett.* **2009**, *38*, 1184–1185.

(14) Liu, Y.; Ishihara, A.; Mitsushima, S.; Kamiya, N.; Ota, K. Zirconium Oxide for PEFC Cathodes. *Electrochim. Solid-State Lett.* **2005**, *8*, A400–A402.

(15) Liu, Y.; Ishihara, A.; Mitsushima, S.; Ota, K. Influence of Sputtering Power on Oxygen Reduction Reaction Activity of Zirconium Oxides Prepared by Radio Frequency Reactive Sputtering. *Electrochim. Acta* **2010**, *55*, 1239–1244.

(16) Liu, Y.; Ishihara, A.; Mitsushima, S.; Kamiya, N.; Ota, K. Transition Metal Oxides as DMFC Cathodes without Platinum. *J. Electrochem. Soc.* **2007**, *154*, B664–B669.

(17) Kim, J.-H.; Ishihara, A.; Mitsushima, S.; Kamiya, N.; Ota, K. Catalytic Activity of Titanium Oxide for Oxygen Reduction Reaction as a Non-Platinum Catalyst for PEFC. *Electrochim. Acta* **2007**, *52*, 2492–2497.

(18) Maekawa, Y.; Ishihara, A.; Mitsushima, S.; Ota, K. Catalytic Activity of Zirconium Oxynitride Prepared by Reactive Sputtering for ORR in Sulfuric Acid. *Electrochim. Solid-State Lett.* **2008**, *11*, B109–B112.

(19) Doi, S.; Ishihara, A.; Mitsushima, S.; Kamiya, N.; Ota, K. Zirconium Based Compounds for New Cathode of Polymer Electrolyte Fuel Cell. *J. Electrochem. Soc.* **2007**, *154*, B362–B369.

(20) Kim, J.-H.; Ishihara, A.; Mitsushima, S.; Kamiya, N.; Ota, K. Oxygen Reduction Reaction of Ta–C–N Prepared by Reactive Sputtering with Heat Treatment. *Electrochemistry* **2007**, *75*, 166–168.

(21) Ishihara, A.; Tamura, M.; Matsuzawa, K.; Mitsushima, S.; Ota, K. *Electrochim. Acta* **2010**, *55*, 7581–7589.

(22) Ishihara, A.; Tamura, M.; Matsuzawa, K.; Mitsushima, S.; Ota, K. Tantalum Oxide-Based Compounds as New Non-Noble Cathodes

for Polymer Electrolyte Fuel Cell. *J. Fuel Cell Sci. Technol.* **2011**, *8*, 031005.

(23) Ohgi, Y.; Ishihara, A.; Matsuzawa, K.; Mitsushima, S.; Matsumoto, M.; Imai, H.; Ota, K. Oxygen Reduction Reaction on Tantalum Oxide-Based Catalysts Prepared from TaC and TaN. *Electrochim. Acta* **2012**, *68*, 192–197.

(24) Ohgi, Y.; Ishihara, A.; Matsuzawa, K.; Mitsushima, S.; Matsumoto, M.; Imai, H.; Ota, K. Factors for Improvements of Catalytic Activity for Zirconium Oxide-Based Oxygen-Reduction Electrocatalysts. *J. Electrochem. Soc.* **2013**, *160*, F162–F167.

(25) Imai, H.; Matsumoto, M.; Miyazaki, T.; Fujieda, S.; Ishihara, A.; Tamura, M.; Ota, K. Structural Defects Working as an Active Oxygen-Reduction Site in Partially Oxidized Ta-Carbonitride Core-Shell Particles Probed by a Surface-Sensitive Conversion-Electron-Yield X-Ray Absorption Spectroscopy. *Appl. Phys. Lett.* **2010**, *96*, 191905.

(26) Schreder, S. L. Towards a 'Universal Curve' for Total Electron-Yield XAS. *Solid. State. Commun.* **1996**, *98*, 405–409.

(27) Shimada, S. A Thermoanalytical Study on the Oxidation of ZrC and HfC Powders with Formation of Carbon. *Solid State Ionics* **2002**, *149*, 319–326.

(28) Shimada, S. Interfacial Reaction on Oxidation of Carbides with Formation of Carbon. *Solid State Ionics* **2001**, *141–142*, 99–104.